# Electrowinning of Copper in a Lab-Scale Squirrel-Cage Cell with Anion Membrane

**L. Cifuentes and R. Ortiz**
Depto. de Ingeniería de Minas, Facultad de Ciencias Físicas y Matemáticas, Universidad de Chile, Tupper 2069, Santiago, Chile

**J. M. Casas**
Depto. de Ingeniería Química, Facultad de Ciencias Físicas y Matemáticas, Universidad de Chile, Beauchef 861, Santiago, Chile

*DOI 10.1002/aic.10476*
*Published online May 23, 2005 in Wiley InterScience (www.interscience.wiley.com).*

*This work describes the design and optimization of a laboratory-scale copper electrowinning cell based on reactive electrodialysis that incorporates a cathode made of copper granules contained in a rotating squirrel-cage–type enclosure. It also incorporates the $Fe^{2+} \rightarrow Fe^{3+} + e$ anodic reaction to overcome the principal disadvantages of conventional electrowinning technology. With this design, anolyte (aqueous $FeSO_4 + H_2SO_4$) and catholyte (aqueous $CuSO_4 + H_2SO_4$) are kept separate by an anion membrane that prevents cation transport between the electrolytes. Experiments were carried out to characterize cell performance under various conditions, and results show that energy requirements with this cell can be 25% lower than conventional industrial values. The same results also show that the squirrel-cage cell can be used to electrowin copper from impoverished electrolytes.* © 2005 American Institute of Chemical Engineers *AIChE J,* 51: 2273–2284, 2005

*Keywords: copper, electrowinning, electrodialysis, particulate bed, squirrel-cage cell*

## Introduction

### *Limitations of conventional copper electrowinning technology*

Although the technology involved in modern solvent extraction and electrowinning (EW) is over 30 years old and despite the fact that electrowinning accounts for almost 1/5 of the world's copper production, there are several major disadvantages associated with copper EW that have never been successfully overcome.

In traditional Cu EW cells, the $Cu^{2+}/Cu^0$ cathodic reaction takes place on square sheet cathodes (height: 1 m, width: 1 m, thickness: 0.1–1 cm) that alternate, side by side, with sheet lead anodes of similar dimensions. The recirculation flow rate is between 10 and 15 $m^3/h$ and the cell volume is about 8 $m^3$. This causes a very low degree of electrolyte agitation in most of the cell volume.

The disadvantages of conventional cells include a low mass-transfer rate to the cathode surface (which in turn limits current density); low specific cathode surface area ($m^2/kg$) and the use of an anodic reaction ($2H_2O \rightarrow O_2 + 4H^+ + 4e$), which requires elevated cell voltages resulting in high energy requirements (2 kWh per kg of deposited Cu); and environmental issues associated with the production of acid mist. Attempts have been made at producing improved cell designs by increasing the mass-transfer rate, using particulate cathodes and replacing the anodic reaction by less energy-demanding reactions. In spite of these efforts, no integral solutions have been proposed. The limitations of conventional cells and attempts at overcoming them have been reviewed by Cifuentes et al.[1]

### *Objectives*

The work described here sets itself two distinct tasks:

(1) To design an alternative copper electrowinning cell that

Correspondence concerning this article should be addressed to L. Cifuentes at luicifue@ing.uchile.cl.

simultaneously overcomes the aforementioned shortcomings of conventional EW technology.

(2) To carry out a series of laboratory-scale experiments to characterize and optimize the kinetics of copper EW using this design.

## Overcoming the Limitations of Conventional Electrowinning Cells

### *Cell designs*

Although modifications of conventional cells have proven useful in reducing cell voltage and increasing current density[2] their drawbacks (such as accelerated corrosion of lead anodes as a result of the dislodging of the oxide layer under ultrasonic agitation, or air sparging and elevated pumping costs associated with forced electrolyte circulation) have limited the use of such adaptations. This in turn has led to the more radical approach of redesigning the Cu electrowinning cell, with particular emphasis placed on large cathode specific surface area and electrolyte agitation.[3] Various authors[2-6] have suggested the use of mesh, particulate bed, or fluidized bed cathodes, although these designs have generally been considered for the recovery of metals from dilute aqueous solutions and not as alternatives to current EW technology.

The use of a particulate bed electrode (PBE) or of a fluidized bed electrode (FBE)—where the particles are smaller and move faster than in the PBE—has two clear advantages, given that these designs promote electrolyte agitation, thereby improving mass transfer, and the bed exhibits a larger specific surface area compared to that of sheet electrodes. However, new electrode types introduce new complications. Shortcomings of the fluidized bed include problems arising from clogging of membranes used in the cell (caused by the small particle sizes involved), uneven potential distribution throughout the bed, and metal deposition on the current feeders.[3,7] A particulate bed cathode, on the other hand, retains most of the advantages of the FBE while eliminating some of its more problematical characteristics. In addition to being simpler than the FBE in terms of design and construction, applications of the PBE such as those reviewed by Kammel[3] feature continuous contact between cathode particles and current feeder, even while maintaining a high degree of agitation. For the reasons listed above the particulate bed cathode was chosen as the basis for the cell developed in this work.

### *Anodic reactions*

The cell voltage can be reduced by means of an alternative anodic reaction that can lead to a lower equilibrium potential difference between the cathodic and anodic reactions and lower anodic overpotential. Several energetically advantageous reactions have been considered,[2,6,8-10] although some of these involve toxic reactants or products, whereas others require expensive chemicals. One particular alternative that has proven favorable in terms of cell voltage without introducing numerous complications is the $Fe^{2+} \rightarrow Fe^{3+} + e$ anodic reaction. In addition to having an equilibrium potential 0.46 V lower than that of the conventional water decomposition reaction, research shows that the ferrous to ferric ion reaction can produce lower anodic overpotentials, provided an adequate anodic material is used.[1] This alternative is also devoid of potentially hazardous or overly expensive reagents. Moreover, the generated ferric ion can be used as an oxidizing agent in combined leaching processes; it may also produce ferric compounds of commercial value.

The presence of the $Fe^{3+}$ ion in Cu EW electrolytes can lead to a drastic reduction of the cathodic current efficiency as a result of the reduction of ferric to ferrous ion on the cathode.[8,9] A practical solution is to separate anolyte and catholyte by using electrodialytic membranes, thereby obtaining specific reactions at both electrodes in a process known as *reactive electrodialysis* (RED). In this case, the $Cu^{2+} + 2e \rightarrow Cu^0$ reaction is to take place in the cathode, whereas the $Fe^{2+} \rightarrow Fe^{3+} + e$ anodic reaction occurs in a separate anodic partition. Recent developments in the application of ED include treatment of solutions from copper electrometallurgy, as well as the thermodynamic modeling of the speciation of these systems.[11-15]

Experimental results show that a laboratory-scale copper electrowinning cell using an anion membrane to separate cathodic and anodic compartments can operate at cell current densities in the 250–400 A/m$^2$ range with cell voltages ranging between 1.0 and 1.9 V, depending on the anode material.[1,13] This suggests that, from an energy consumption perspective, a design based on RED with a ferrous ion anolyte is able to perform better than conventional Cu EW technology, which is characterized by cell current densities in the 250–350 A/m$^2$ range with cell voltages $\cong$ 2 V. However, energy is not the only variable to be considered in a full comparison between the performance of a new cell design and conventional technology (see Conclusions).

### *Anode materials*

The criteria for selecting anode materials must consider anodic kinetics as well as more practical aspects. Cifuentes et al.[1] recently investigated the effectiveness of several anode materials for the ferrous to ferric ion reaction. In the cited study, potentiodynamic experiments were carried out using lead sheet (Pb), platinum sheet (Pt), platinum on titanium mesh (Pt/Ti), ruthenium bioxide on titanium mesh ($RuO_2$/Ti), iridium bioxide on titanium mesh ($IrO_2$/Ti), and graphite. Cell voltages were measured in a RED cell using each material in turn but otherwise operating under identical experimental conditions, allowing a direct comparison of their efficacy as catalysts for the $Fe^{2+} \rightarrow Fe^{3+} + e$ anodic reaction. Pb did not catalyze the studied reaction, but the remaining materials did. Table 1 shows that, under the conditions studied, the reaction is fastest on Pt, whereas the performances of Pt/Ti, $RuO_2$/Ti, $IrO_2$/Ti, and graphite are satisfactory and not substantially different.

Based on the aforementioned results, graphite bar anodes were chosen for the RED cell developed in this work. The decision was based on the performance shown by graphite anodes as well as its unit cost, which is lower than that of the alternatives.

## Experimental Methodology

### *Cell and cathode design*

In accordance with the findings relating to overcoming the limitations of conventional electrowinning cells, it was decided to incorporate the following key elements in the design:

**Table 1. Reactive Electrodialysis Cell Voltage (in V) for Three Cell Current Densities and Five Anode Materials**

| $i_{cell}$ (A/m$^2$) | Pt | Pt/Ti | $RuO_2$/Ti | $IrO_2$/Ti | Graphite |
|---|---|---|---|---|---|
| 400 | 1.73 | 1.93 | 1.92 | 2.02 | 1.93 |
| 250 | 1.17 | 1.30 | 1.36 | 1.38 | 1.33 |
| 200 | 0.99 | 1.14 | 1.18 | 1.18 | 1.14 |

*Average value over 3-h tests. From Cifuentes et al.[1]

- Separate compartments for cathode/catholyte and anode/anolyte.
- Particulate bed cathode consisting of Cu particles between 1 and 3 mm in diameter, with a proper current feeder system.
- Use of graphite bar anodes catalyzing the $Fe^{2+}/Fe^{3+}$ anodic reaction.
- Incorporation of agitation mechanisms for both catholyte and anolyte.

The squirrel-cage RED cell design is a direct result of the need to fulfill these objectives in the simplest way possible, while adapting to laboratory conditions. The cell is a batch reactor that incorporates 1800 cm$^3$ double-jacket recirculation tanks for both anolyte and catholyte to increase electrolyte capacity and maintain constant temperature. As previously stated, the design incorporates a particulate bed cathode in combination with graphite anodes catalyzing the ferrous to ferric ion reaction. The use of anion membranes permits the separation of a Fe(II) anolyte from a copper EW type catholyte. A side-by-side layout was chosen for the anodic and cathodic compartments (Figure 1) because of the simplicity of assembling and disassembling the cell when using this arrangement. Both compartments are made of 18-mm-thick acrylic sheet, a material that shows high stability in the presence of moderate concentrations of sulfuric acid and temperatures up to 70°C. The two box-shaped sections are linked by a 12 × 13-cm opening. The effective compartment volume is 975 cm$^3$ in both cases. Both compartments are separated by an anion membrane. The anode consists of 30 partially submerged graphite bars (diameter: 4.85 mm; length: 200 mm). These are placed vertically and are wired together with 0.5-mm copper wire in their exposed upper ends. The apparent submerged anode surface area was 550 cm$^2$. Cifuentes et al.[1] determined that the effective surface area of the graphite rods is 26% greater than its apparent surface area, which gives a corrected figure of 690 cm$^2$ for these anodes.

The copper granules that constitute the cathode are contained in a cylindrical enclosure intended to rotate about its central axis (a "squirrel cage"). This cathode assembly was designed to provide agitation as well as to serve as a current feeder for the particles, given that the cage's drive axle is also the main cathode bus bar (Figure 2). The cage consists of a polymeric frame and covering mesh that minimizes both weight and exposed conducting surfaces. Its internal measurements are 10 cm in diameter and 1.5 cm in thickness, and internal volume is about 115 cm$^3$. Metallic current feeders are connected to the drive axle (see Figure 2). They also allow for the lifting of the granulated copper mass during the rotation of the squirrel cage. Two graphite brushes, placed on the external part of the axle, provide the electrical connection to the power supply. The bus bar/drive axle was fashioned from cylindrical copper stock to improve conductivity with the carbon brush assembly. A variable-speed electric motor drives the cage through a polyamide pinion situated on the external part of the axle.

The anode–membrane and cathode–membrane distances were 3 cm each, so that the anode–cathode separation was 6 cm.

### *Cell operation*

The studied variables were current density ($i_{cell}$, A/m$^2$ referenced to the apparent membrane surface area), temperature (°C), electrolyte flow rate (cm$^3$/min), cathode particle type (granules or wire segments), cathode mass (g), and Cu concentration in the catholyte (g/L). The cell's performance was evaluated by comparing cell voltage ($V_{cell}$, V), current efficiency (CE), and specific energy consumption (SEC, kWh/kg) under different conditions. Anolyte/catholyte compositions and basic experimental conditions were determined for cell operation (Table 2). Electrolytes were prepared using analytical-quality $CuSO_4 \cdot 5H_2O$, $FeSO_4 \cdot 7H_2O$, and $H_2SO_4$. A cell rotation velocity of 30 rpm was used as a standard condition, as was a temperature of 50°C, which is similar to that of conventional EW operations. Power was provided by a 20-A, 30-V Idisa rectifier.

To separate anolyte from catholyte an Ionac MA3475 anion membrane was fitted between both compartments. Membranes were conditioned twice, for 24 h each time, in an agitated beaker filled with a 190 g/L $H_2SO_4$ solution at 25°C, and were disposed of after each use. The membranes were kept in place by two 2-mm-thick rubber seals that left an exposed membrane

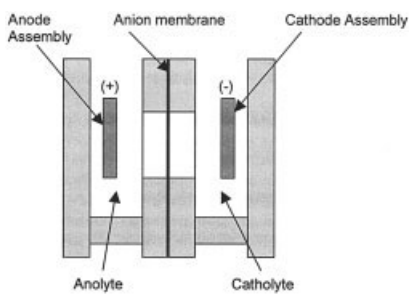


**Figure 1. Cell layout.**

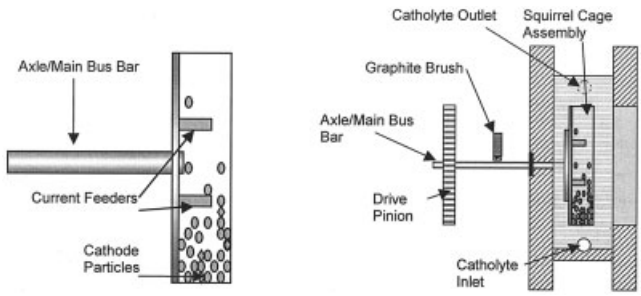


**Figure 2. Squirrel-cage cathode assembly.**

**Table 2. Electrolyte Properties under Standard Conditions**

| Electrolyte | Electrolyte Composition (g/L) | | | Temperature (°C) | Flow Rate ($cm^3$/min) |
|---|---|---|---|---|---|
| | $[Cu^{2+}]$ | $[Fe^{2+}]$ | $[H_2SO_4]$ | | |
| Catholyte | 40.0 | 0 | 190 | 50 | 900 |
| Anolyte | 0 | 55.8 | 190 | 50 | 900 |

surface of 10 × 10 cm. The entire cell was held together by 11 stainless steel bars bolted at both ends. Recirculation of the electrolytes was carried out by two Watson–Marlow 505S peristaltic pumps, and additional agitation was provided by means of a Stuart Scientific SS3 stirrer in the anodic compartment (equipped with a 3-cm-diameter impeller) and by the rotation of the squirrel cage in the cathodic compartment. Total volumes for anolyte and catholyte were 2000 $cm^3$ each. Two double-jacket 1800 $cm^3$ recirculation glass tanks were used and the temperature of both electrolytes was kept constant by means of a Julabo thermostatic bath. Cell voltage was measured at rectifier connection points by means of a Fluke model 179 multimeter. Cell current was given by the rectifier itself with a precision of 0.1 A.

Under standard operating conditions the cage was filled with 400 g of granulated copper that, having an apparent density of 5.13 g/$cm^3$, constitutes 2/3 of the cage's internal volume. The apparent density is defined as bulk mass/apparent volume. The apparent volume is measured by means of a graduated cylinder and it includes the empty volume between copper granules. As a result, the apparent density is smaller than the density of a solid copper block. Standard electrolyte conditions are as listed in Table 2.

Three experimental protocols were devised to compare the results obtained from operating under different conditions:

(1) Current density ($i_{cell}$) sweeps to determine $V_{cell}$ for the $i_{cell}$ range available (300 to 1800 A/$m^2$).

(2) Cu deposition at constant current density for a total of 3 h, with the objective of comparing deposition mass with applied current and thus calculating current efficiency and power consumption.

(3) Cell voltage vs. cage rotation speed (rpm).

Tests were carried out using a total of 15 combinations of the experimental variables. Conditions for all tests are shown in Table 3, where items in boldface type represent deviations from standard conditions.

### *Cell voltage and specific energy consumption*

The principal operational indicators are current efficiency, cell voltage, and specific energy consumption. Current efficiency was obtained by using Faraday's equation to relate deposition mass to applied cell current

$$\frac{m_F}{eq} = \frac{I \cdot t}{F} \tag{1}$$

where the equivalent weight is $eq = 63.546/2$ for the $Cu^{2+}/Cu^0$ cathodic reaction.

Current efficiency (CE) is thus obtained as the relationship between Cu mass given by Faraday's equation ($m_F$) and total deposition mass ($m_T$), measured as the cathode assembly weight difference before and after the experiment

$$\mathrm{CE} = \frac{m_T}{m_F} \tag{2}$$

Another important parameter is current efficiency for deposition on the particulate cathode ($CE_P$), which does not consider copper deposition on the current feeders

$$\mathrm{CE}_P = \frac{m_P}{m_F} \tag{3}$$

Here $m_P$ is the weight difference of the cathode particles before and after deposition.

Specific energy consumption (SEC) considering all Cu deposition, in kWh/kg Cu, is given by

$$\mathrm{SEC} = \frac{V_{cell} I t}{m_T} = \frac{F}{3600 eq} \frac{V_{cell}}{\mathrm{CE}} \tag{4}$$

**Table 3. Experimental Conditions**

| $i_{cell}$* (A/$m^2$) | $T$ (°C) | $[Cu^{2+}]$ (g/L) | Flow Rate ($cm^3$/min) | Cathode Type | Cathode Mass (g) | Experimental Protocol** |
|---|---|---|---|---|---|---|
| 1000 | 50 | 40 | 900 | Granular | 400 | 1, 2, 3 |
| 1000 | **22** | 40 | 900 | Granular | 400 | 1, 2, 3 |
| 1000 | **35** | 40 | 900 | Granular | 400 | 1, 2, 3 |
| 1000 | 50 | 40 | **500** | Granular | 400 | 1, 2, 3 |
| 1000 | 50 | 40 | **1470** | Granular | 400 | 1, 2, 3 |
| 1000 | 50 | 40 | 900 | Granular | **200** | 1, 2, 3 |
| 1000 | 50 | 40 | 900 | Granular | **600** | 1, 2, 3 |
| 1000 | 50 | 40 | 900 | **1 mm wire** | **200** | 1, 2, 3 |
| 1000 | 50 | 40 | 900 | **1 mm wire** | 400 | 1, 2, 3 |
| 1000 | 50 | **10** | 900 | Granular | 400 | 1, 2, 3 |
| **500** | 50 | 40 | 900 | Granular | 400 | 1, 2, 3 |
| n/a | 50 | 40 | 900 | **Cu sheet** | n/a | 1 |
| n/a | 50 | **10** | 900 | **Cu sheet** | n/a | 1 |

*Cell current density (referred to apparent membrane surface area) used during prolonged deposition.
**Indicates which protocols were carried out under each set of conditions: 1 = current density sweep; 2 = prolonged deposition at constant $i_{cell}$; 3 = $V_{cell}$ vs. rpm.

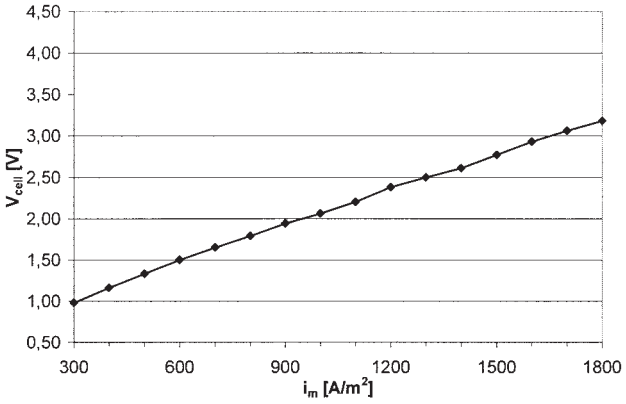


**Figure 3. Cell voltage vs. cell current density for base conditions.**

$T$ = 50°C, [$Cu^{2+}$] = 40 g/L, $Q$ = 900 $cm^3$/min, cathode = 400 g of granular type.

Thus, SEC is a function of average cell voltage $V_{cell}$ (during deposition at constant cell current $I$) and CE.

If deposition on current feeders is not considered, the specific energy consumption for deposition on the particulate cathode is

$$\mathrm{SEC}_P = \frac{V_{\mathrm{cell}} I t}{m_P} = \frac{F}{3600 eq} \frac{V_{\mathrm{cell}}}{\mathrm{CE}_P} \tag{5}$$

## Results and Discussion

### *Cell current*

Experiments show that anodic and cathodic current densities have the greatest effect on cell voltage and thus on energy requirements. As Figure 3 shows, under standard conditions the cell voltage exceeded 2 V at current densities $>$ 930 A/$m^2$. Current efficiency did not substantially change and specific energy consumption decreased from 1.67 to 1.06 kWh/kg when the cell current density decreased from 1000 to 500 A/$m^2$ (Table 4). This represents a 37% improvement in energy efficiency with a 50% decrease in production rate.

If one examines the components of cell voltage (Eq. 6), the potential drop in anolyte, catholyte, and membrane as well the anodic and cathodic overpotentials all increase with cell current

$$V_{\mathrm{cell}} = \Delta E_e + \eta_a + |\eta_c| + (IR)_a + (IR)_c + (IR)_m + p \tag{6}$$

The standard equilibrium potentials at 25°C are 0.34 V for the cupric/copper reaction and 0.77 V for the ferrous/ferric reaction, both against SHE (standard hydrogen electrode). The equilibrium potential for the anodic reaction ($E_{e,a}$) at 50°C was found to increase from an initial value of 0.67 to 0.78 V (average value = 0.73 V) as the $Fe^{3+}/Fe^{2+}$ ratio in the anolyte increased, whereas the equilibrium potential for the cathodic reaction at 50°C remained at 0.33 V. Thus the average equilibrium potential difference during the experiment was 0.40 V.

Whereas the electrolyte and membrane potential drops increase proportionally with $I$, overpotentials do so according to Eqs. 8 and 9 derived from Fick's law for mass-transfer control, a high-field approximation to the Butler–Volmer equation for charge-transfer control, and a relationship that links them both

$$\frac{1}{i_{\mathrm{MC}}} = \frac{1}{i_{\mathrm{CTC}}} + \frac{1}{i_{\mathrm{MTC}}} \tag{7}$$

In Eq. 7, $i_{MTC}$, the current density under mass-transfer control, corresponds to the limiting current density $i_L$.

In normal electrodialysis reversal (EDR) cell operation, both reactions (cupric ion reduction and ferrous ion oxidation) are under mixed control. As a function of cell current $I$ and electrode surface area $S$, the resulting expressions for the overpotentials are, for an anodic reaction under mixed control

$$\eta_a = \frac{-RT}{\alpha_a F} \ln\left[ i_{0,a}\left(\frac{S_a}{I} - \frac{1}{i_{L,a}}\right)\right] \tag{8}$$

and, for a cathodic reaction under mixed control

$$|\eta_c| = \frac{RT}{\alpha_c F} \ln\left[ i_{0,c}\left(\frac{S_c}{I} - \frac{1}{|i_{L,c}|}\right)\right] \tag{9}$$

Given that the effective anode surface area is 690 $cm^2$, under standard conditions ($I$ = 10 A) the anodic current density is 145 A/$m^2$. The value of the limiting current density for the $Fe^{2+}/Fe^{3+}$ reaction ($i_{L,a}$) was found to be 390 A/$m^2$. Using values for $\alpha_a$ and $i_{0,a}$ obtained under similar conditions[1] the anodic overpotential given by Eq. 8 is 0.34 V. This suggests that the $Fe^{2+}/Fe^{3+}$ anodic reaction always takes place under mixed control, as was previously assumed.

Electrolyte resistance, on the other hand, can be obtained from the following equation

$$R = \left(\frac{d}{a}\right)\frac{1}{\kappa} \tag{10}$$

Cifuentes et al.[1,13] provide average values for the conductivity of electrolytes of the type used in this work

$$\text{Anolyte} \qquad \kappa_{a,50^\circ\mathrm{C}} = 76.5\ \Omega^{-1}\, m^{-1}$$

$$\text{Catholyte} \qquad \kappa_{c,50^\circ\mathrm{C}} = 73.9\ \Omega^{-1}\, m^{-1}$$

Equation 10 applies to a standard sheet electrode cell with a fixed electrode distance $d$. For the squirrel-cage cell, individual electrolyte resistances can be obtained by considering the anode–membrane distance ($d_a$) and cathode–membrane distance ($d_c$), approximately 3 cm each. The area ($a$) used in Eq. 10 was

**Table 4. Operational Indicators for Deposition at 1000 and 500 A/$m^2$ ***

| $i_{\mathrm{cell}}$ (A/$m^2$) | $V_{\mathrm{cell}}$** (V) | CE (%) | SEC (kWh/kg Cu) |
|---|---|---|---|
| 1000 | 1.91 | 96.7 | 1.67 |
| 500 | 1.21 | 96.7 | 1.06 |

*Conditions: $T$ = 50°C, [$Cu^{2+}$] = 40 g/L, $Q$ = 900 $cm^3$/min, cathode = 400 g of granular type. CE, current efficiency; SEC, specific energy consumption.

**Average cell voltage while operating at constant $i_{\mathrm{cell}}$.

**Table 5. Cell Voltage ($V_{cell}$, $V$) Quantification for Deposition at 1000 A/m$^2$ under Standard Conditions***

| $\Delta E_e$** | $\eta_a$** | $\lvert\eta_c\rvert$** | $(IR_\Omega)_a$** | $(IR_\Omega)_c$** | $(IR_\Omega)_m$** | $p^\dagger$ | Total |
|---|---|---|---|---|---|---|---|
| 0.40 | 0.34 | 0.10 | 0.37 | 0.41 | 0.30 | 0.05 | 1.97 |

*$T$ = 50°C, [$Cu^{2+}$] = 40 g/L, $Q$ = 900 cm$^3$/min, cathode = 400 g of granular type, $d_{ac}$ = 6 cm.
**From Cifuentes et al.[1,16]
†Measured.

that of the membrane, 0.01 m$^2$. The resistances thus obtained were 0.039 Ω for the anolyte and 0.041 Ω for the catholyte. Combined, these are accountable for 0.8 V (42%) of the cell voltage at 1000 A/m$^2$ under standard conditions.

The conductivity of both electrolytes should vary with pH, given that the $H^+$ ion exhibits the highest mobility and diffusivity, but measurements indicated that the pH varies by only about 0.01 units during the tests. This is because no $H^+$ or $OH^-$ ions are produced or consumed by the anodic and cathodic reactions during normal cell operation. In other words, pH variations do not contribute in a significant measure to cell voltage variations.

Because the electrolytes are agitated, the assumption has been made that they are well mixed, so that there are no significant concentration gradients that could alter the conductivity and, as a result, there is no dependency of the conductivity on the Reynolds number.

Cifuentes et al.[1,13] measured a 0.15-V potential drop across an Ionac MA3475 membrane when operating under similar conditions at 500 A/m$^2$. This extrapolates to 0.30 V when operating at 1000 A/m$^2$, under standard conditions.

The term $p$ for various voltage drops deals mainly with the effect of the resistance of the anode and cathode assemblies. Because of the difficulty of obtaining dependable resistance values of the various cell components, potential differences while operating at 10 A were measured instead. Several such measurements showed that an average voltage drop of 40 mV occurs between anode bars and the anode assembly connecting wire, whereas an additional voltage drop of 10 mV occurs between the cathode connecting point and the drive axle. This means that the total assembly resistance is only about 0.005 Ω and therefore it accounts for about 2.5% of cell voltage under standard operating conditions. This term does not include the apparent resistivity of the particulate bed.

Table 5 shows a breakdown of the cell voltage for the squirrel-cage cell operating under standard conditions. The experimental value of $V_{cell}$ (1.91 V, Table 4) is slightly lower than the value obtained from published data (1.97 V, Table 5).

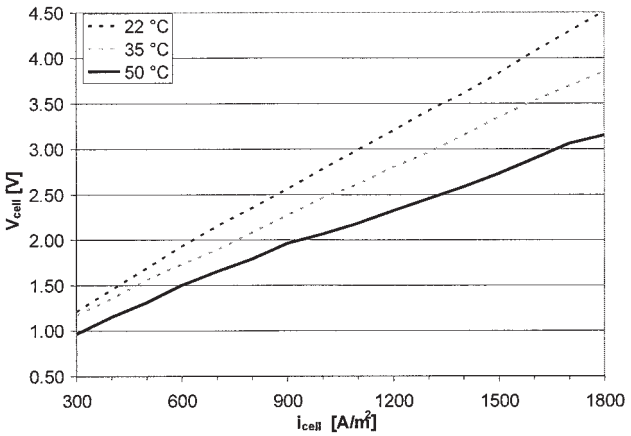


**Figure 4. Cell voltage vs. cell current density for 22, 35, and 50°C.**

[$Cu^{2+}$] = 40 g/L, $Q$ = 900 cm$^3$/min, cathode = 400 g of granular type.

### *Temperature*

An increase in electrolyte temperature can be expected to affect mass transport by means of increased ion mobilities and diffusivities as well as a lower viscosity, which in turn improves convective and diffusive transport. The effect on cell performance is shown in Figure 4, where there is a clear relationship between temperature increase and cell voltage reduction. The same is true for specific energy consumption (Table 6), which is lowest for 50°C.

### *Cathode mass and cathode type*

The granulated copper used for the cathode consists of regular-shaped particles (Figure 5), 94% of which are between 1 and 5 mm in diameter. Apparent density (defined above) is 5.13 g/cm$^3$. An alternative cathode material consisting of 1-mm-diameter copper wire, cut into 1-cm segments, was also tested. The chopped wire has a homogeneous length distribution, ranging from 0.8 to 1.5 cm, and an apparent density of 2.66 g/cm$^3$. Because of the narrow size ranges involved, both particle distributions were obtained through photographic analysis.

Tests were carried out using 200, 400, and 600 g of granular cathode. Increasing cathode mass has a two-pronged effect on the charge-transfer characteristics of the cell. The cathode surface area increases in direct proportion with cathode mass. In addition to this, electrical contact between cathode particles improves when the cage is filled so that cathodization of particles can be expected to be more efficient with greater cathode mass. Experimental results show that an increase of granular cathode of 200 g results in a decrease in cell voltage of 0.1 V (Figure 6).

Chopped wire cathode proved less adequate from an energetic perspective than its granular counterpart, causing a 0.25 V increase in average cell voltage. This was associated with an

**Table 6. Operational Indicators for Deposition at Various Electrolyte Temperatures***

| $T$ (°C) | $V_{cell}$** (V) | CE (%) | SEC (kWh/kg Cu) |
|---|---|---|---|
| 22 | 2.69 | 95.8 | 2.37 |
| 35 | 2.29 | 95.2 | 2.03 |
| 50 | 1.91 | 96.7 | 1.67 |

*Conditions: [$Cu^{2+}$] = 40 g/L, $Q$ = 900 cm$^3$/min, cathode = 400 g of granular type. CE, current efficiency; SEC, specific energy consumption.
**Average cell voltage while operating at $i_{cell}$ = 1000 A/m$^2$.

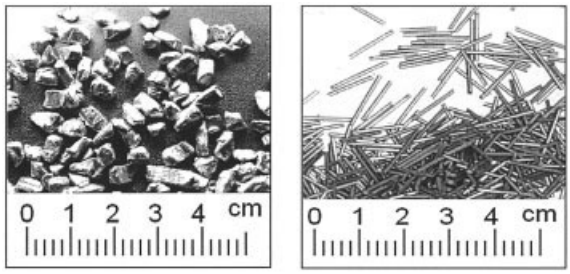


**Figure 5. Granular (left) and chopped wire (right) cathode particles.**

increase in specific energy consumption of 9 and 13% for 200 and 400 g of cathode, respectively (Table 7).

For cell optimization under varying conditions, current efficiency (CE) and specific energy consumption (SEC) are calculated considering total copper deposition. An exception is made when changing cathode mass and type because these variables have a direct effect on the percentage of copper deposition on the current feeders. For this reason, current efficiency for Cu deposition on the particulate bed ($CE_P$) and specific energy consumption for Cu deposition on the particulate bed ($SEC_P$) must also be compared.

Deposition on the current feeders was as high as 28.1% when 200 g of granular cathode were used vs. an unwanted deposition of only 2.6% for the same mass of chopped wire (Table 8). Unwanted deposition on current feeders increases when these are not obscured by cathode particles and are directly exposed to the electric field. This explains why unwanted deposition decreases with increasing cathode mass, and is partially responsible for the better performance of the chopped wire, which has a lower apparent density (and thus occupies more of the cage's internal volume). In addition to this the chopped wire is more abrasive than the well-rounded granular cathode type. This is important because abrasion will also hinder deposition on the fixed-current feeders.

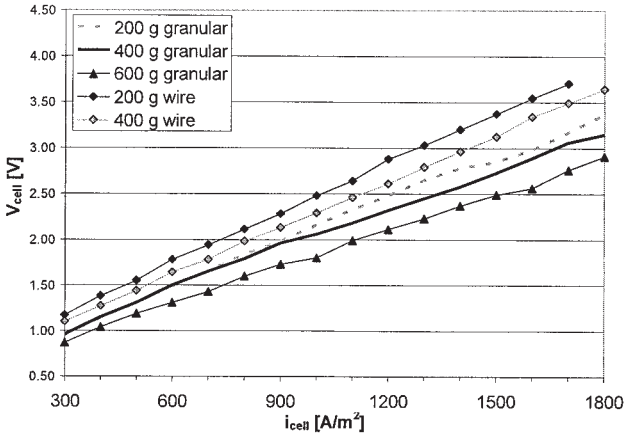


**Figure 6. Cell voltage vs. cell current density for different cathode masses and types.**

$i_{cell}$ = 1000 A/m$^2$, $T$ = 50°C, [$Cu^{2+}$] = 40 g/L, $Q$ = 900 cm$^3$/min.

**Table 7. Operational Indicators for Various Cathode Types and Masses***

| Cathode Type | Cathode Mass (g) | $V_{cell}$** (V) | CE (%) | SEC (kWh/kg Cu) |
|---|---|---|---|---|
| Granular | 200 | 1.97 | 96.2 | 1.73 |
| Granular | 400 | 1.91 | 96.7 | 1.67 |
| Granular | 600 | 1.79 | 99.3 | 1.52 |
| Chopped wire | 200 | 2.23 | 99.4 | 1.89 |
| Chopped wire | 400 | 2.12 | 97.6 | 1.83 |

*Conditions: $T$ = 50°C, [$Cu^{2+}$] = 40 g/L, $Q$ = 900 cm$^3$/min. CE, current efficiency; SEC, specific energy consumption.
**Average cell voltage while operating at $i_{cell}$ = 1000 A/m$^2$.

### *Electrolyte recirculation*

Tests were carried out using three different electrolyte flow rates (Table 9). Electrode reaction rates increase with the degree of forced convection caused by mechanical agitation and recirculation of the electrolyte. This is to be expected because the thickness of the diffusion layer ($\delta$), which forms next to the electrode surface, diminishes with increasing agitation, so that the limiting current density ($i_L$) increases according to Fick's law

$$i_L = zFD\frac{c_b}{\delta} = zFkC_b \tag{11}$$

Changes in electrolyte circulation flow rate proved relevant in the 500 to 900 cm$^3$/min range, but had a negligible effect when increased from 900 to 1470 cm$^3$/min (Figure 7). Electrolyte recirculation is not the only source of forced convection, however. The anodic compartment is provided with a stirrer, which lessens the contribution of anolyte recirculation. On the other hand, although the rotating cathode assembly provides some agitation of the catholyte, it is this part of the cell that benefits most from recirculation because the squirrel cage normally rotates at a slow speed (30 rpm). The mesh that covers the cage, however, provides an obstruction to electrolyte flow and probably accounts for the lack of improvement beyond 900 cm$^3$/min.

### *Cage rotation speed*

Experimental data in Figure 8 provide insight as to how the rotation speed of the squirrel cage affects both the charge-transfer and mass-transfer characteristics of the cathode. If rotation is slow (<70 rpm) the particles settle to the bottom, thus improving contact with the current feeders, which leads to

**Table 8. Effect of Cathode Mass Type on Cu Deposition on Current Feeders***

| Cathode Type | Mass (g) | Deposition on CF (%) | $CE_P$** (%) | $SEC_P$** (kWh/kg Cu) |
|---|---|---|---|---|
| Granular | 200 | 28.1 | 69.2 | 2.40 |
| Granular | 400 | 6.8 | 90.2 | 1.79 |
| Granular | 600 | 2.6 | 96.7 | 1.56 |
| Chopper wire | 200 | 2.6 | 96.8 | 1.94 |
| Chopper wire | 400 | 1.6 | 96.1 | 1.86 |

*Conditions: $T$ = 50°C, [$Cu^{2+}$] = 40 g/L, $Q$ = 900 cm$^3$/min.
**$CE_P$, current efficiency for deposition on particulate cathode; $SEC_P$, specific energy consumption for deposition on particulate cathode.

**Table 9. Operational Indicators for Deposition at Various Electrolyte Flow Rates***

| Flow Rate ($cm^3$/min) | $V_{cell}$** (V) | CE (%) | SEC (kWh/kg Cu) |
|---|---|---|---|
| 500 | 2.07 | 97.5 | 1.79 |
| 900 | 1.91 | 96.7 | 1.67 |
| 1470 | 1.89 | 97.8 | 1.63 |

*Conditions: $T$ = 50°C, $[Cu^{2+}]$ = 40 g/L, cathode = 400 g of granular type. CE, current efficiency; SEC, specific energy consumption.
**Average cell voltage while operating at $i_{cell}$ = 1000 A/$m^2$.

a better potential distribution throughout the cathode and a decrease in cell voltage (this corresponds to the $V_{cell}$ minimum in Figure 8). At fast rotation speeds (>150 rpm) the particles are driven together by centrifugal force, forming a packed ring inside the cylinder, which produces a similar effect to that of slow rotation, but with better mass transfer resulting from the high agitation and thus a $V_{cell}$ minimum generally occurs in this region. Intermediate velocities lead to a cascade-type flow of the cathode particles, with intermittent contact with the current feeders and a corresponding decline in cell performance (manifested as the maximum cell voltage in the curves in Figure 8) stemming from the poorer cathodization of the particulate bed.

Although the previous results suggest high rotation speeds to be advantageous, continued operation under such conditions led to a packing of the electrode particles with a subsequent deterioration of mass-transfer characteristics and an early onset of limiting current density as the Cu concentration in the catholyte decreased. In addition to this, there is the practical consideration of handling a solid-packed cathode mass. For these reasons, a cage rotation speed of 30 rpm was chosen.

The effects of cage rotation speed are different under varying flow rates and cathode types. When recirculation is low, the cathode's mass-transfer capabilities become more dependent on cell rotation (its only other source of forced convection) and the difference between maximum and minimum $V_{cell}$ is widest, as shown by the first data series in Figure 8.

The curves corresponding to high recirculation and low recirculation (first and third data series in Figure 8) are closest together at high cage rotation speeds, where cage rotation

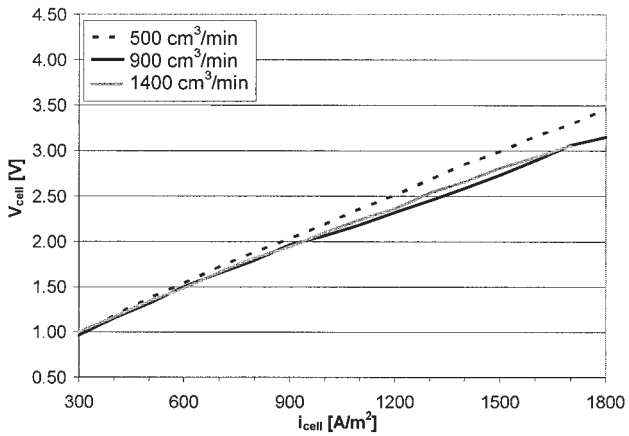


**Figure 7. Cell voltage vs. cell current density for 500, 900, and 1470 $cm^3$/min recirculation flow rates.**

$T$ = 50°C, $[Cu^{2+}]$ = 40 g/L, cathode = 400 g of granular type.

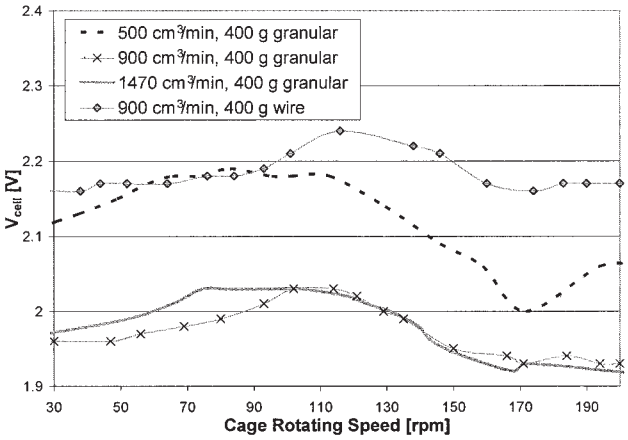


**Figure 8. Cell voltage vs. cage rotation speed for various flow rates and cathode types.**

$i_{cell}$ = 1000 A/$m^2$, $T$ = 50°C, $[Cu^{2+}]$ = 40 g/L.

provides most of the agitation and the flow rate difference is least relevant. The opposite is true for low rotation speeds.

Results show that, when using a chopped-wire cathode, the cell voltage is least dependent on cell rotation speed. This type of material has a lower apparent density and when 400 g are used the wire takes up most of the cage's internal volume. This suggests that the movement characteristics of the chopped wire remain largely unchanged throughout the studied velocity range.

### *Copper concentration and limiting current density*

To obtain information on the mass-transfer capabilities of the particulate electrode two experiments were carried out, with catholyte Cu concentrations of 10 and 40 g/L, using a sheet cathode of dimensions similar to those of the squirrel-cage assembly. The sheet cathode consists of a 0.5-mm-thick copper disc with a diameter of 11.3 cm. The disc was fastened to the end of the drive axle, where the squirrel cage would normally be mounted. The back of the disc was coated with epoxy resin, leaving a total cathode surface area of 100 $cm^2$ facing the membrane. Agitation was provided (as with the squirrel cage), by rotating the disc at 30 rpm.

At $[Cu^{2+}]$ = 40 g/L the sheet cathode presented better performance up to a membrane current density of 925 A/$m^2$ (Figure 9). Beyond that point the cell voltage with the sheet cathode became substantially higher than that with the particulate electrode and hydrogen evolution was observed at 1300 A/$m^2$, signaling the limiting current density for the $Cu^{2+}/Cu^0$ reaction.

When the catholyte copper concentration was reduced to 10 g/L, the sheet cathode outperformed the particulate cathode only at current densities between 300 and 500 A/$m^2$, and a limiting current density for the $Cu^{2+}/Cu^0$ reaction on the sheet cathode was reached between 500 and 600 A/$m^2$.

The previous findings indicate that, when the rate-determining step for the $Cu^{2+}/Cu^0$ cathodic reaction is charge transfer (or when the electrode potential is in the mixed control range but closer to charge-transfer control), the sheet electrode is preferable because of its more uniform potential distribution. One must keep in mind that the particulate cathode is charac-

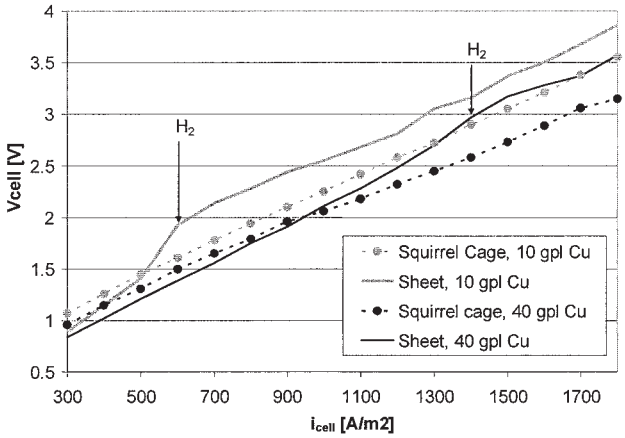


**Figure 9. Cell voltage vs. cell current density for sheet cathode and squirrel-cage assembly, operating with catholyte Cu concentrations of 10 and 40 g/L.**

$T = 50°C$, $Q = 900$ cm$^3$/min. $H_2$ denotes hydrogen evolution (only on sheet cathode).

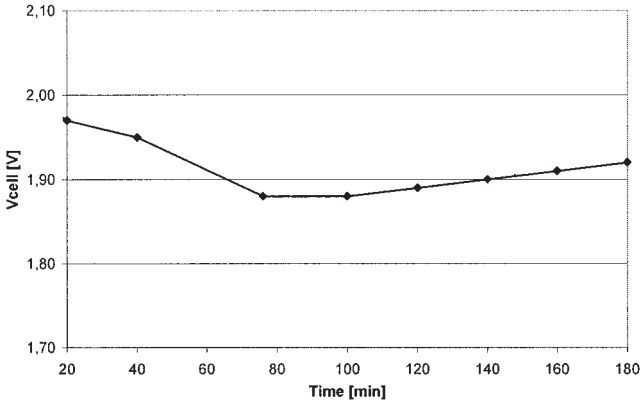


**Figure 10. Cell voltage vs. time of operation at constant $i_{cell}$ = 1000 A/m$^2$ under standard conditions.**

$[Cu^{2+}] = 40$ g/L, $T = 50°C$, $Q = 900$ cm$^3$/min, cathode = 400 g granular.

terized by a potential distribution where the cathodic potential of the current feeders is shared only by those particles in direct or indirect contact with them.

When mass transfer becomes a relevant factor at elevated current densities, the particulate cathode is preferable to the sheet cathode. The squirrel-cage cathode shows adequate performance throughout the tested $i_{cell}$ range, and independent test runs place the limiting current density for the $Cu^{2+}/Cu^0$ reaction at >2500 A/m$^2$ under standard conditions compared to 1300 A/m$^2$ with the sheet cathode. The use of a catholyte with a copper concentration of 10 g/L provides further proof. Here the sheet cathode was altogether ineffective, whereas the squirrel cage allowed a sustained cell operation at 1000 A/m$^2$ with Cu concentration in the catholyte becoming as low as 0.5 g/L toward the end of the experiment, despite which specific energy consumption was <2 kWh/kg Cu (Table 10). This is largely explained by the fact that the $H^+/H_2$ cathodic reaction did not occur until the end of the experiment and total current efficiency was as high as 95.8%.

### *Cell voltage and specific energy consumption: comparison with conventional electrowinning cells*

The behavior of cell voltage over time while operating at constant membrane current density, under standard conditions, is shown in Figure 10. The cell voltage decreases during the first 80 min of cell operation and then it slowly increases. This behavior can be explained in terms of five effects:

(1) An initial increase in the conductivity of the membrane as it absorbs ions (other than $H^+$ and $SO_4^=$) from both electrolytes. This effect, which implies a reduction in cell voltage, ceases when the membrane becomes saturated.

(2) A decrease in catholyte conductivity as cupric ions are slowly depleted by copper electrodeposition. This effect leads to a steady cell voltage increase.

(3) An increase in anolyte conductivity as the oxidation of ferrous ions gives rise to ferric ions and the $[Fe^{3+}]/[Fe^{2+}]$ ratio increases. This effect results in a steady cell voltage decrease.

(4) A decrease in the concentration of ferrous ions, which causes a decrease in the production rate of ferric ions, leading to a decrease of both the exchange current density ($i_0$) and the limiting current density ($i_L$) of the anodic reaction. These phenomena produce a steady increase in the anodic overpotential and, therefore, in the cell voltage.

(5) A decrease in the concentration of cupric ions, which causes a decrease in the exchange current density and the limiting current density of the cupric ion reduction reaction, which steadily increases the cathodic overpotential and, therefore, the cell voltage.

Two of these effects tend to reduce the cell voltage, one permanently (3) and one temporarily (1) at the start of the operation, whereas the remaining three effects (2, 4, and 5) tend to permanently increase it. The overall result of these five effects is that the cell voltage first decreases after which it gradually increases.

Current efficiency and specific energy consumption thus far consider all Cu deposition, with the exception of the analysis dealing with the effects of different cathode types and mass. The gap between total current efficiency (CE) and current efficiency for deposition on the particulate bed ($CE_P$) is indicative of the amount of unwanted deposition on the current feeders. It averaged 6.5% under standard conditions.

Taking this into account the squirrel-cage cell nonetheless outperforms current copper EW technology by a significant margin, particularly when dealing with depleted electrolytes. Under standard conditions specific energy consumption of the particulate deposit was 1.79 vs. 2 kWh/kg for conventional electrowinning cells. Table 11 lists all experimental conditions for which $CE_P$ was <2 kWh/kg Cu (where as in Table 3 items in boldface type represent deviations from standard conditions)

**Table 10. Operational Indicators for Two Cu Concentrations in the Catholyte***

| $[Cu^{2+}]$ (g/L) | $V_{cell}$** (V) | CE (%) | SEC (kWh/kg Cu) |
|---|---|---|---|
| 10 | 2.24 | 95.8 | 1.98 |
| 40 | 1.91 | 96.7 | 1.67 |

*Conditions: $T = 50°C$, $Q = 900$ cm$^3$/min, cathode = 400 g of granular type. CE, current efficiency; SEC, specific energy consumption.
**Average cell voltage while operating at $i_{cell} = 1000$ A/m$^2$.

**Table 11. Experimental Conditions Leading to Low Specific Energy Consumptions for the Production of Particulate Deposits***

| $i_{cell}$ (A/m$^2$) | $T$ (°C) | [$Cu^{2+}$] (g/L) | Flow Rate (cm$^3$/min) | Cathode Type | Mass (g) | $V_{cell}$** (V) | $CE_P$ (%) | $SEC_P$ (kWh/kg) |
|---|---|---|---|---|---|---|---|---|
| 1000 | 50 | 40 | 900 | Granular | 400 | 1.91 | 90.2 | 1.79 |
| 1000 | 50 | 40 | 900 | Granular | **600** | 1.79 | 96.7 | 1.56 |
| 1000 | 50 | 40 | 900 | **1 mm wire** | **200** | 2.23 | 96.8 | 1.94 |
| 1000 | 50 | 40 | 900 | **1 mm wire** | 400 | 2.12 | 96.1 | 1.86 |
| 1000 | 50 | 40 | **1470** | Granular | 400 | 1.89 | 90.4 | 1.77 |
| **500** | 50 | 40 | 900 | Granular | 400 | 1.21 | 82.0 | 1.25 |

*$CE_P$, current efficiency for deposition on particulate cathode. $SEC_P$, specific energy consumption for deposition on particulate cathode.
**Average cell voltage while operating at constant $i_{cell}$.

and the corresponding cell current sweeps are shown in Figure 11.

When a catholyte containing 10 g/L Cu was used, $SEC_P$ reached a value of 2.06 kWh/kg Cu, which is comparable to that of conventional EW cells operating with an electrolyte containing 40 g/L Cu. In addition to being energetically more efficient, the aforementioned result corresponds to the squirrel-cage cell operating at a current density of 1000 A/m$^2$. Under such conditions, the same cell operating with a sheet cathode was able to attain only 500 A/m$^2$ before the appearance of a limiting current density for the $Cu^{2+}/Cu^0$ reaction.

### *Comments on scale-up*

The present study did not include experimental scale-up of the squirrel-cage cell. It should be pointed out that, among the components of the cell voltage (Eq. 6), the overpotentials of the anodic and cathodic reactions, as well as the ohmic drop across the membrane, depend on current density and are independent of the size of the reactor, provided that the electrolyte composition and the temperature remain unchanged. The equilibrium potential difference does not vary with cell size either because the electrochemical system would remain the same. Thus only the potential drops in anolyte and catholite are direct functions of cell geometry, that is, functions of the distance between anode and cathode (cathode–membrane plus anode–membrane), factors that should be considered in an eventual scale-up of the squirrel-cage cell.

Table 12 shows the effect of the anode–cathode distance ($d_{ac}$) on the cell voltage. If the distance on scale-up could be reduced from 6 cm (Table 5) to 1 cm, the cell voltage would decrease from 1.97 to 1.32 V (a 33% decrease). On the other hand, if $d_{ac}$ increased from 6 to 10 cm, the cell voltage would increase from 1.97 to 2.49 V (a 26% increase). This shows the importance of cell dimensions on the energy requirements to drive the cell.

An additional contribution to the cell voltage depends on the frequency of granule–feeder and granule–granule contacts inside the squirrel cage. This term was discussed above and is represented in Figure 8. It is likely to vary with the cage size, the overall mass of granules, and the cage rotation speed, so its effect on scale-up should be experimentally determined.

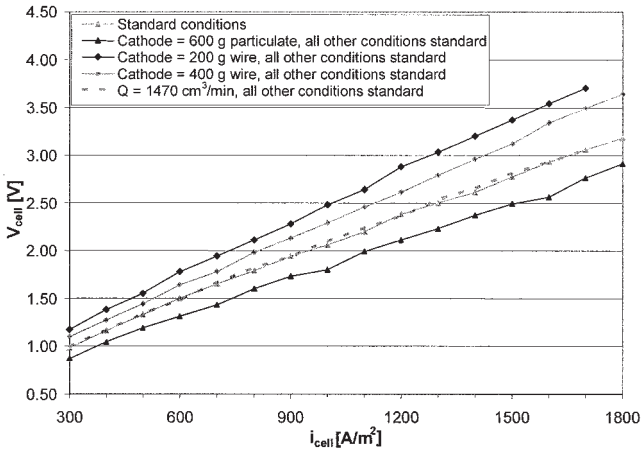


**Figure 11. Cell voltage vs. cell current density.**

Standard conditions: [$Cu^{2+}$] = 40 g/L, $T$ = 50°C, $Q$ = 900 cm$^3$/min, $i_{cell}$ = 1000 A/m$^2$, cathode = 400 g particulate.

## Conclusions

Among the operational variables considered in this work, those most relevant to the energy efficiency of the squirrel-cage cell in terms of cell voltage and specific energy consumption are electrolyte temperature, cathode mass and type, $Cu^{2+}$ concentration in the catholyte, and operating current density. Electrolyte flow rate has a less significant effect that becomes irrelevant above 900 cm$^3$/min. Cage rotation speed, on the other hand, produces variations in $V_{cell}$ that are only <0.1 V for the studied conditions.

Current efficiency (CE) ranged from 95.2 to 99.4% and appears to be adversely affected by a decrease in temperature. For experiments carried out at 50 °C and [$Cu^{2+}$] = 40 g/L, CE averaged 97.5%.

Current efficiency for Cu deposition on the particles ($CE_P$) follows the same tendencies as CE but it is always lower, given that $CE_P$ does not consider the copper deposition on the current feeders (which is about 7% under standard conditions). The difference between CE and $CE_P$ was lowest for the wire cathode because of its abrasive nature (which results in continual removal of Cu deposit on the current feeders) as well as its higher apparent volume, which allows it to mask the current feeders. On the other hand, $CE_P$ was lowest when using 200 g of particulate cathode because the low volume of the particle bed left the feeders highly exposed to unwanted Cu deposition.

Specific energy consumption (SEC) averaged 1.67 kWh/kg Cu under standard conditions. SEC is a function of cell voltage and current efficiency and, because CE showed little variation throughout, the differences in SEC arose from dissimilarities in cell voltages. For operations at 1000 A/m$^2$, the SEC was worst (2.37 kWh/kg Cu) when electrolyte temperature was reduced to 22°C, and reached its best value (1.52 kWh/kg Cu) when using a 50% greater mass of particulate cathode.

It is necessary to put the performance of the squirrel-cage

Table 12. Cell Voltage ($V_{cell}$) Quantification for Deposition at 1000 A/m$^2$ for Two Anode–Cathode Distances ($d_{ac} = d_a + d_c$)*

| $d_{ac}$ (cm) | $\Delta E_e$ (V) | $\eta_a$ (V) | $\lvert\eta_c\rvert$ (V) | $(IR_\Omega)_a$ (V) | $(IR_\Omega)_c$ (V) | $(IR_\Omega)_m$ (V) | $p$ (V) | Total (V) |
|---|---|---|---|---|---|---|---|---|
| 1 | 0.40 | 0.34 | 0.10 | 0.06 | 0.07 | 0.30 | 0.05 | 1.32 |
| 10 | 0.40 | 0.34 | 0.10 | 0.60 | 0.70 | 0.30 | 0.05 | 2.49 |

*Note:* Based on data from Table 5.
*Conditions: $T = 50$°C, $[Cu^{2+}] = 40$ g/L, $Q = 900$ cm$^3$/min, cathode = 400 g of granular type.

cell into context to compare it with conventional Cu electrowinning technology. The $SEC_P$ for tests carried out under standard conditions averaged 1.79 kWh/kg Cu and unwanted copper deposition on current feeders was limited to about 7%. When using the maximum amount (600 g) of particulate cathode, $SEC_P$ reached its lowest value of 1.56 kWh/kg Cu. This is substantially lower than the 2 kWh/kg Cu typical of conventional Cu electrowinning operations. However, energy consumption is not the only significant variable in copper electrowinning. A full comparison between the performance of the squirrel-cage cell and conventional technology should include a study of the effect of impurities on cathode quality, pilot-scale testing, economic analysis, and other considerations. Further work is needed before such comparison can be made.

The squirrel-cage cell benefits greatly from operating with a nearly full cathode cage because of a greater cathode surface area, a more efficient cathodization of Cu particles, and a drastic reduction of Cu deposition on the current feeders, all of which have a positive effect on energy requirements. Changing (1) the shape of the cathode particles and (2) the cathode–anode distance can also have very significant effects on cell performance.

## Acknowledgments

This work was funded by the National Committee for Scientific and Technological Research (CONICYT, Chile) through FONDECYT Project No. 101 0138. Thanks are due to Gloria Crisóstomo and Pablo Arriagada for their help with the experimental work and fruitful discussions; to the Mining Engineering and Chemical Engineering Departments, Universidad de Chile, for their continuous support; and to Placer Dome for financial aid to the Chair of Environmental Studies in Mining.

## Notation

$a$ = apparent membrane surface area, m$^2$
$c_b$ = bulk concentration, mol L$^{-1}$
CE = current efficiency, %
$CE_P$ = current efficiency for Cu deposition on the particulate bed, %
$d$ = thickness of compartment, m
$d_{ac}$ = anode–cathode distance = $d_a + d_c$
$d_a$ = anode–membrane distance, m
$d_c$ = cathode–membrane distance, m
$D$ = diffusivity, m$^2$ s$^{-1}$
$E_e$ = equilibrium potential, V
$\Delta E_e$ = difference between $E_e$ values of anodic and cathodic reactions, V
$F$ = Faraday's constant, C eq$^{-1}$
$i_{cell}$ = cell current density measured over membrane surface area, A m$^{-2}$
$i_{CTC}$ = electrode current density under charge-transfer control, A m$^{-2}$
$i_{MTC}$ = electrode current density under mass-transfer control, A m$^{-2}$
$i_{MC}$ = electrode current density under mixed control, A m$^{-2}$
$i_L$, $i_{L,a}$, $i_{L,c}$ = limiting current density, anodic, and cathodic, A m$^{-2}$
$i_0$, $i_{0,a}$, $i_{0,c}$ = exchange current density, anodic, and cathodic, A m$^{-2}$
$I$ = cell current, A
$(IR)_a$ = potential drop in anolyte, V
$(IR)_c$ = potential drop in catholyte, V
$(IR)_m$ = potential drop in membrane, V
$k$ = mass-transfer coefficient, m s$^{-1}$
$m_F$ = Cu deposition mass at 100% current efficiency, kg
$m_P$ = mass of Cu deposition on particulate bed, kg
$m_T$ = mass of Cu deposition on particulate bed and current feeders, kg
$p$ = other undesired potential drops, V
$Q$ = electrolyte flow rate, cm$^3$/min
$R$ = electrical resistance, Ω
$S$, $S_a$, $S_c$ = electrode surface area, anode, and cathode, m$^2$
SEC = specific energy consumption, kWh/kg Cu
$SEC_P$ = specific energy consumption for Cu deposition on the particulate bed, kWh/kg Cu
$t$ = time of operation, s
$T$ = temperature, K
$V_{cell}$ = cell voltage, V
$z$ = charge number

### *Greek letters*

$\alpha_a$ = anodic charge-transfer coefficient
$\alpha_c$ = cathodic charge-transfer coefficient
$\delta$ = thickness of the diffusion layer, m
$\eta$, $\eta_a$, $\eta_c$ = overpotential, anodic, and cathodic, V
$\kappa$, $\kappa_a$, $\kappa_c$ = electrical conductivity, anolyte, and catholyte, Ω$^{-1}$ m$^{-1}$

## Literature Cited

1. Cifuentes L, Glasner R, Casas JM. Aspects of the development of a copper electrowinning cell based on reactive electrodialysis. *Chem Eng Sci*. 2004;59:1087-1101.
2. Cooper WC. Advances and future prospects in copper electrowinning. *J Appl Electrochem*. 1985;15:789-805.
3. Kammel R. Metal recovery from dilute aqueous solutions by various electrochemical reactors. In: Bautista RA, ed. *Hydrometallurgical Process Fundamentals*. New York, NY: Plenum Press; 1982:617-648.
4. Fleischmann M, Oldfield JW. Fluidised bed electrodes: Part I. Polarisation by simplified models. *J Electroanal Chem*. 1971;29:211-230.
5. Fleischmann M, Oldfield JW. Fluidised bed electrodes: Part II. The effective resistivity of the discontinuous metal phase. *J Electroanal Chem*. 1971;29:231-248.
6. Spring KA, Evans JW. An investigation of sulphite ion oxidation as an alternative anode reaction in fluidized bed electrowinning or other high rate electrolysis cells. *J Appl Electrochem*. 1984;15:609-618.
7. Gabrielli C, Huet F, Sahar A. Dynamic analysis of charge transport in fluidized bed electrodes; impedance techniques for electro-inactive beds. *J Appl Electrochem*. 1992;22:801-809.
8. Dew DW. The effect of Fe(II) and Fe(III) on the efficiency of copper electrowinning from dilute acid Cu(II) sulphate solutions with the Chemelec cell. Part I. Cathodic and anodic polarization studies. *Hydrometallurgy*. 1985;14:331-349.
9. Dew DW. The effect of Fe(II) and Fe(III) on the efficiency of copper electrowinning from dilute acid Cu(II) sulphate solutions with the Chemelec cell. Part II. The efficiency of copper electrowinning from dilute liquors. *Hydrometallurgy*. 1985;14:351-367.
10. Sandoval SP. A substitute anode for electrowinning copper. In: Cooper WC, ed. Proc of COPPER'95 Int Conf, Vol. III, Electrorefining and hydrometallurgy of copper. Toronto, Canada: The Metallurgical Society of the Canadian Institute of Mining, Metallurgy and Petroleum; 1995:423-435.
11. Cifuentes L, Crisóstomo G, Alvarez F, Casas J, Cifuentes G. The use

of electrodialysis for separating and concentrating chemical species in acidic Cu-Fe-As-Sb electrolytes. In: Dutrizac J, Ji J, Ramanachandran V, eds. Proc of COPPER'99 4th Int Conf, Vol. 3, Electrorefining and electrowinning. Phoenix, AZ: TMS Publishers; 1999:479-493.
12. Cifuentes L, Crisóstomo G, Ibáñez JP, Casas JM, Alvarez F, Cifuentes G. On the electrodialysis of aqueous $H_2SO_4$–$CuSO_4$ electrolytes with metallic impurities. *J Membr Sci*. 2002;207:1-16.
13. Cifuentes L, Castro JM, Casas JM. Modeling a copper electrowinning cell based on reactive electrodialysis. Unpublished results; 2004.
14. Casas JM, Alvarez F, Cifuentes L. Aqueous speciation of $H_2SO_4$–$CuSO_4$ solutions. *Chem Eng Sci*. 2000;55:6223-6234.
15. Casas JM, Crisóstomo G, Cifuentes L. Aqueous speciation of electrowinning solutions. In: Riveros PA, ed. Proc of COPPER 2003 5th Int Conf, Vol. VI, Copper electrorefining and electrowinning, Book 1. Phoenix, AZ: TMS Publishers; 2003:441-456.
16. Cifuentes L, Simpson J. Temperature dependence of the cathodic kinetics in a membrane-based copper electrowinning cell. Unpublished results; 2004.

*Manuscript received Mar. 19, 2004, and revision received Dec. 6, 2004.*